

Electronic Shell Structure and Abundances of Sodium Clusters

W. D. Knight

*Department of Physics, University of California, Berkeley, California 94720,^(a)
and Clarendon Laboratory, Oxford OX1 3PU, United Kingdom*

and

Keith Clemenger, Walt A. de Heer, and Winston A. Saunders

Department of Physics, University of California, Berkeley, California 94720

and

M. Y. Chou and Marvin L. Cohen

*Department of Physics, University of California, Berkeley, California 94720, and Materials and Molecular Research Division,
Lawrence Berkeley Laboratory, Berkeley, California 94720*

(Received 12 April 1984)

Mass spectra are presented for sodium clusters of N atoms per cluster ($N = 4-100$) produced in a supersonic expansion with argon carrier gas. The spectra show large peaks or steps at $N = 8, 20, 40, 58,$ and 92 . These can be understood in terms of a one-electron shell model in which independent delocalized atomic $3s$ electrons are bound in a spherically symmetric potential well.

PACS numbers: 36.40.+d, 31.20.-d, 35.20.Wg

We find distinct regularities in the mass spectra of sodium clusters containing between $N = 2$ and $N = 100$ sodium atoms per cluster. Figure 1(a) shows a single continuous mass scan over the range $N = 4-75$, and a separate mass scan for $N = 75-100$. Each peak represents the number of clusters of a given N detected during a fixed time interval in a molecular beam of sodium seeded in argon. The peaks or steps for certain masses, corresponding to $N = 8, 20, 40, 58,$ and 92 , are conspicuously large, especially compared with the peaks immediately following. The dimer, $N = 2$ (not shown), also exhibits pronounced abundance relative to $N = 3-7$. Between the above peaks we observe uniquely patterned regions which are recognizable over a wide range of experimental conditions. For example, the even-odd alternations in the ranges $N = 8-14$ and $N = 34-40$ are always seen regardless of the relative intensities of the respective whole regions. To illustrate this, Fig. 2 shows mass scans for four different argon pressures and a constant sodium vapor pressure of 16 kPa. It may be seen that increasing pressure favors the large clusters, and causes depletion of the smaller ones, without altering the integrities of the respective regions. The clusters which are conspicuously abundant in the mass spectra are assumed to be relatively more stable. If we furthermore single out the electronic structure of those clusters as the cause of the enhanced stability, a simple picture emerges.

We associate the main sequence $N = 8, 20, 40,$

$58,$ and 92 with an electronic shell structure for sodium clusters. The shell structure is determined by large energy gaps between different energy levels. The electronic structure of bulk sodium metal can be understood by using the nearly free-electron picture. In this case, the $3s$ valence electron interacts with a smooth one-particle effective potential composed of ionic pseudopotentials and an electron-electron interaction potential.¹ A similar model appears to be applicable to the clusters. We simulate the effective one-electron potential inside the cluster with a spherically symmetric rounded potential well. The calculation is performed with a potential of the form

$$U(r) = - \frac{U_0}{\exp[(r - r_0)/\epsilon] + 1}, \quad (1)$$

where U_0 is the sum of the Fermi energy (3.23 eV) and the work function (2.7 eV)² of the bulk³; r_0 is the effective radius of the cluster sphere and assumed to be $r_s N^{1/3}$, where r_s is the radius of a sphere containing one electron in the bulk ($r_s = 3.93$ a.u. for sodium). The parameter ϵ determines the variation of the potential at the edge of the sphere. We use $\epsilon = 1.5$ a.u. in this calculation, which is consistent with the results from the self-consistent study of the jellium surface.⁴

The Schrödinger equation is solved numerically for each N . It yields discrete electronic energy levels characterized by the angular momentum quantum number L with degeneracy $2(2L + 1)$ (includ-

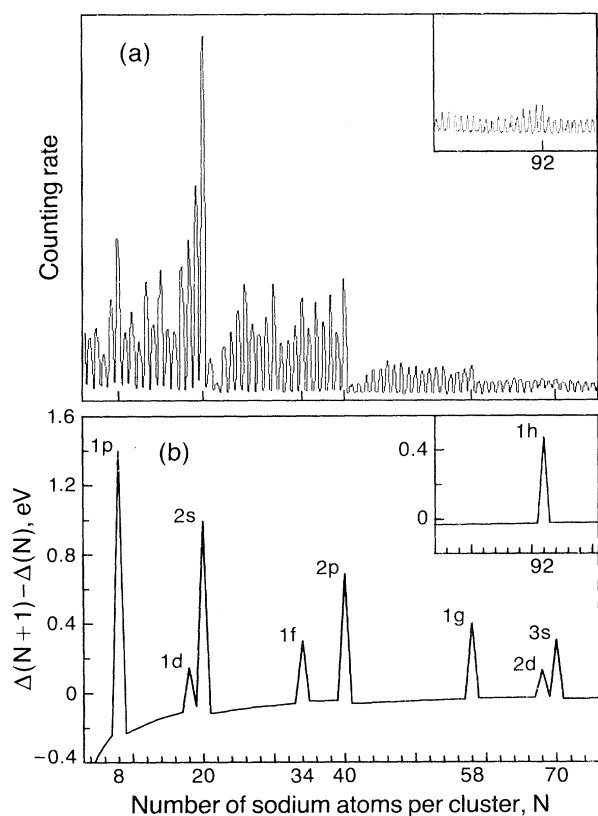


FIG. 1. (a) Mass spectrum of sodium clusters, $N = 4-75$. The full scale intensity in the main figure is approximately 20 000 counts/sec. Source conditions: $P_{Ar} = 750$ kPa, $P_{Na} = 24$ kPa. The inset corresponds to $N = 75-100$. (b) The calculated change in the electronic energy difference, $\Delta(N+1) - \Delta(N)$ (see text), vs N . The labels of the peaks correspond to the closed-shell orbitals.

ing spin). The energy levels shift down slowly and continuously as N increases. The electronic energy for each cluster with N atoms, $E(N)$, is obtained by summing the eigenvalues of the occupied states. The difference in electronic energy between adjacent clusters, $E(N) - E(N-1)$, is defined as $\Delta(N)$. The change in this quantity versus N is plotted in Fig. 1(b). Peaks result when $\Delta(N+1)$ increases discontinuously, as an energy level is just filled at certain N and the next orbital starts to be occupied in the cluster with $N+1$ atoms. We expect that the contribution to the binding energy from the ion-ion electrostatic energy is a smooth function versus N , therefore the discontinuities in the electronic energy should remain in the total binding energy of clusters.

The shell-closing numbers (the peak positions) mark positions of steps in the binding energy and these correspond to steps in the measured abun-

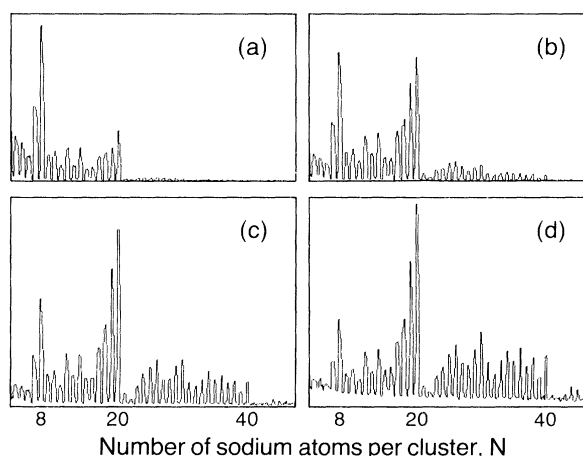


FIG. 2. Sodium-cluster mass spectra ($N = 4-47$) for varying carrier-gas pressure P_{Ar} at constant sodium vapor pressure 16 kPa. (a) $P_{Ar} = 300$ kPa, (b) $P_{Ar} = 400$ kPa, (c) $P_{Ar} = 500$ kPa, and (d) $P_{Ar} = 600$ kPa.

dances as seen in Fig. 1(a). Other peaks found in the calculation at $N = 18, 34, 68,$ and 70 are weaker than the observed ones and are more sensitive to the potential parameter.⁵ The good correspondence between the experiment results and the model calculation suggests that there are no perturbations large enough to distort the main features of the level structure. We conclude that the peaks or steps at special numbers in the sodium-cluster mass spectra result from the electronic properties. This is in contrast to the explanation of the reported observations of "magic numbers" using structural packing patterns for noble-gas clusters.⁶⁻⁹

The molecular-beam source¹⁰ is loaded with high-purity sodium (without the use of oils or solvents) from an argon-filled glovebox which is connected to the source chamber. This procedure insures a high degree of cleanliness and accounts for the fact that the 0.076-mm-diam nozzle is free of plugging. The stainless-steel source may be operated at temperatures up to 1200 K and at argon pressure exceeding 10^6 Pa. A heated 0.375-mm-diam skimmer lies approximately 1 cm downstream of the nozzle. The clusters are ionized 2 m downstream by light from a 1-kW Hg-Xe lamp. The light is filtered with Corning 9863 glass. Our quadrupole mass analyzer (QMA) is mounted coaxially with the beam axis, and all cluster ions enter paraxially. The ions are mass selected by the QMA and are detected with a Daly ion-detection system,¹¹ which has single-ion counting capability. The aluminum Daly dynode is at a potential of -25 kV. The maximum range of the QMA is 4500 amu and the mass acceptance width is set at approximately 5 amu over the

entire range. The counts resulting from individual ions are stored in a multichannel analyzer (MCA). The QMA mass-scanning voltage ramps are generated by an LSI-11 computer, which also controls the channel advance of the MCA. The mass spectra in the figures are unprocessed reproductions of the counts stored in the MCA.

Related, but different, results have been reported¹² for sodium clusters. These workers observe four distinct abundance maxima in their mass spectra at $N=2, 7, 19,$ and 38 . The differences between our and their results are understandable. As noted in Ref. 12, the placing of the QMA axis normal to the beam distorts the mass spectrometer acceptance function. Also they point out the desirability of working with a cold beam, but for a seeded beam with their high ($\sim 25\%$) concentration of sodium vapor the quoted temperatures are not possible.^{13,14} Our vapor concentrations are only a few percent, and time-of-flight measurements show speed ratios of between 7 and 10 in all cases, indicating considerable cooling of the beam.

We have performed tests to verify that the mass spectra are determined by the cluster production. We found that using different filters in the uv ionizing light caused no substantial changes in the characteristic features of the mass spectra. Investigation also ruled out the existence of discontinuities in the mass sensitivity of the Daly ion detector and the QMA. The background gas in the vacuum system is primarily argon originating from the source. It is evident from the mass spectra at several different gas pressures (Fig. 2) that selective scattering from this background is not a significant effect. These arguments support our conclusion that the peaks and discontinuities in the mass spectra result from properties intrinsic to the clusters themselves, as reflected in the production process. The cluster binding energy is expected to be important in this process.⁷

Since the observations are consistent with the characteristics of a spherical potential, this suggests that the optical spectra of metal clusters may turn out to be simpler than had been expected. It may also be inferred that the average energy gap in these systems is closer to $E_F/N^{1/3}$ (Ref. 15) than to E_F/N (Ref. 16).

Further experiments are in progress to explore other properties of sodium clusters. We anticipate that these measurements will suggest further refinements in the theoretical approach which will result in improved models for a variety of metallic clusters over a wide range of sizes.

We wish to thank Frank Lopez for his excellent

machining of much of our apparatus. We acknowledge the contributions of R. Monot, W. H. Gerber, E. Dietz, and A. R. George in developing the molecular-beam machine. This work is supported in part by the Materials Research Division of the U. S. National Science Foundation under Grant No. DMR81-15540. One of us (W.D.K.) acknowledges support from the Miller Institute for Basic Research in Science. This work is further supported in part by the National Science Foundation under Grant No. DMR83-19024 and by the Director, Office of Energy Research, Office of Basic Energy Sciences, Material Sciences Division of the U. S. Department of Energy under Contract No. DE-AC03-76SF00098.

(a)Permanent address.

¹N. W. Ashcroft and N. D. Mermin, *Solid State Physics* (Holt, Rinehart and Winston, New York, 1976), pp. 285-288; S. G. Louie, S. Froyen, and M. L. Cohen, *Phys. Rev. B* **26**, 1738 (1982).

²R. L. Gerlach and T. N. Rhodin, *Surf. Sci.* **19**, 403 (1970); Table IV in N. D. Lang and W. Kohn, *Phys. Rev. B* **1**, 4555 (1970).

³We have tested different U_0 for the range $5 \text{ eV} < U_0 < 6 \text{ eV}$ and there are no significant changes in the characteristic features.

⁴Lang and Kohn, Ref. 2. The effective potential near the surface of $r_s = 4 \text{ a.u.}$ jellium in Table I of this reference is close to a potential of the form (1) with $\epsilon = 1.8 \text{ a.u.}$ and $U_0 = 6.18 \text{ eV}$.

⁵In the jellium surface calculation (Lang and Kohn, Ref. 2), the effective surface for electrons is shifted outward from the real jellium surface. If we choose r_0 in (1) as $N^{1/3}r_s$ plus a constant term, the resulting peaks in Fig. 1(b) at $N = 68$ and 70 become smaller.

⁶P. W. Stephens and J. G. King, *Phys. Rev. Lett.* **51**, 1538 (1983).

⁷O. Echt, K. Sattler, and E. Recknagel, *Phys. Rev. Lett.* **47**, 1121 (1981).

⁸A. Ding and J. Hesslich, *Chem. Phys. Lett.* **94**, 54 (1983).

⁹J. A. Barker, *J. Phys. (Paris), Colloq.* **38**, C2-37 (1977).

¹⁰W. A. de Heer, to be published: this source is in principle equivalent to that used in R. A. Larsen, S. K. Neoh, and D. R. Herschbach, *Rev. Sci. Instrum.* **45**, 1511 (1974).

¹¹N. R. Daly, *Rev. Sci. Instrum.* **31**, 264 (1960).

¹²M. M. Kappes, R. W. Kunz, and E. Schumacher, *Chem. Phys. Lett.* **91**, 413 (1982).

¹³J. B. Anderson, *Entropie* **18**, 33 (1967).

¹⁴Larsen, Neoh, and Herschbach, Ref. 10.

¹⁵D. M. Wood and N. W. Ashcroft, *Phys. Rev. B* **25**, 6255 (1982).

¹⁶R. Kubo, *J. Phys. Soc. Jpn.* **17**, 975 (1962).